inter.noise
21-24 AUGUST
SCOTTISH EVENT CAMPUS
GLASGOW 2022

A Boundary Element Method (BEM) solver for low frequency room modes

Andrea Cicero[1]
Acoustics Research Group
Newton Building, University of Salford – Salford M5 4WT – United Kingdom
AC Acustica – Acoustic Design
Viale del Fante, 8 – 97100 Ragusa - Italy

Jonathan A. Hargreaves[2]
Acoustics Research Group
Newton Building, University of Salford – Salford M5 4WT – United Kingdom

ABSTRACT

Room modes are known to be problematic in small critical listening environments. They degrade the acoustic quality at low frequencies, producing peaks and nulls in the frequency domain and ringing in the time domain. The Finite Element Method (FEM) is currently the easiest way to predict such resonances for arbitrarily shaped rooms. This solves for mode frequencies and shapes, as well as Q-factors and decay rates. Such 'eigenfrequency' solvers are commonplace in FEM, but FEM has the disadvantage of needing to mesh the entire air volume in the room. The Boundary Element Method (BEM) avoids this and only requires a simple boundary mesh, but the solution to its eigenfrequency problems is much more challenging and appears in only a few academic papers. Here we transfer those approaches to Room Acoustics. We implement the block Sakurai-Sugiura method, which uses a contour integral in the complex frequency plane to convert the BEM eigenfrequency problem, which is usually non-linear in wavenumber, into a standard linear eigenfrequency problem that is straightforward to solve. The method is demonstrated through application to a cuboid room and an irregularly shaped room, both with impedance boundary conditions. Results are validated against FEM and discussed.

1. INTRODUCTION

Critical listening environments are typically set up in small spaces. All spaces possess acoustic modes, but smaller dimensions push the lowest order modes up into a frequency range where they have a perceptible effect. These resonances can be sparse in frequency and have high Q-factors, so have a strong effect on the perceived acoustic quality of the sonic reproduced material.

Studies based on listening tests [1–4] have highlighted the importance of temporal characteristics of the room resonances. This is quantified by the modal decay time, which is related to Q-factor. They provide perceptual thresholds based on this, rather than the more usual objective parameters such as a controlled modal density or a flat steady-state frequency response.

[1] a.cicero@edu.salford.ac.uk, a.cicero@ac-acustica.it
[2] j.a.hargreaves@salford.ac.uk

Closed-form solutions for resonant modes exist only for simple geometries: spheres, cylinders, cuboids, etc. For arbitrary-shaped rooms, it is necessary to make use of numerical methods such as the Finite Element Method (FEM) to solve for modes frequencies and shapes and related temporal features. These are commonly referred to as 'eigenfrequency' solvers since they rely on eigenmode decomposition of the FEM system matrix. The resonant frequencies are related to the matrix eigenvalues, so are called the eigenfrequencies, and the eigenmodes are the room mode shapes.

The modal decay time is controlled primarily by the amount of absorption present on the boundary surfaces, i.e., the walls of the room under evaluation. This causes the eigenfrequencies to become complex, as explained in the next section, with their imaginary part quantifying the decay rate. Complex eigenfrequencies are therefore useful in room design because they can quantify both the frequency at which modal artefacts occur and how slowly decaying / high Q they are.

This benefit was reported by Magalotti and Cardinali [5], who used complex eigenfrequencies computed with FEM. They additionally used measured modal decay times to calibrate FEM models of various rooms by adjusting the impedance values at the boundaries, obtaining good agreement with the experimental data despite some simplifying assumptions on model configuration.

This paper extends this approach by reporting a method for the modal analysis of small rooms using the Boundary Element Method (BEM). This has the benefit over FEM that only the boundary needs to be meshed, resulting in simpler meshes and fewer degrees of freedom to solve for. However, with BEM it has traditionally only been possible to solve for Frequency Response Results, being the response of the room to time-harmonic excitation by a source at a range of specified frequencies [6]. This contains modal artefacts as peaks but extracting their modes shapes and Q-factors is non-trivial.

Eigenfrequency studies are straightforward in FEM because frequency appears in the matrix equation as a polynomial term, which can be solved for using standard matrix eigenvalue solvers. In BEM, in contrast, frequency is embedded in the matrix entries within a complex exponential, making the eigenfrequency problem non-linear. Recent developments in applied mathematics, however, now mean these problems are solvable and in this work we transfer those techniques to room acoustics.

Another benefit of computing eigenfrequencies in BEM is that it does not suffer from *pollution error*. This is inherent to FEM and describes a dispersion (or phase) error that builds up as a wave propagates through a mesh. This is akin to a stiffening effect that increases the numerical wave speed at higher frequencies. In an eigenfrequency problem, where mode shape wavelength is fixed by the geometry, this manifests as an overestimation of the eigenfrequencies. It has been suggested that pollution error occurs in BEM too [7] but this claim has recently been disproven [8]. In our judgement, the results in [7] most likely are caused by leakage through the mesh due to imperfect reflection.

Section 2 reports the theoretical background and numerical formulation. Section 3 presents results for cuboid and irregular rooms including a comparison with analytical results and FEM. Finally, Section 4 draws conclusions.

2. THEORY AND IMPLEMENTATION

2.1. Modal Decomposition, Complex Eigenfrequencies and Modal Decay

Real sound fields contain many frequencies, but for simplicity, we will analyse a time-harmonic pressure field with a single angular frequency ω. This can be represented as follows:

$$p(\mathbf{x}, t) = \mathrm{Real}\big(P(\mathbf{x}, \omega)\mathrm{e}^{-\mathrm{i}\omega t}\big). \tag{1}$$

Here $p(\mathbf{x}, t)$ is time-dependent pressure, which is real-valued and is what we hear. $P(\mathbf{x}, \omega)$ is the position-dependent complex amplitude of the pressure field; $|P(\mathbf{x}, \omega)|$ is its magnitude and $\angle P(\mathbf{x}, \omega)$ is its relative phase. The $\mathrm{e}^{-\mathrm{i}\omega t}$ term is responsible for the time-harmonic oscillation. $P(\mathbf{x}, \omega)$ satisfies the Helmholtz equation, in which $k = 2\pi f / c_0$ is the wavenumber and c_0 is the speed of sound:

$$\nabla^2 P + k^2 P = 0. \tag{2}$$

In a frequency-domain study, the driving frequency ω is dictated by the user. A frequency sweep is performed to obtain the room transfer function (RTF). But in an eigenfrequency study, the solver finds both $P(\mathbf{x}, \omega)$ and ω, subject to conditions imposed by the geometry and boundary conditions. These are 'natural' modes of the space and are self-sustaining in the absence of a driving signal except for oscillation and an exponential decay if damping is present. The solver will return a set of these solution pairs (mode shapes and frequencies), which we index with a subscript n. It is also common nomenclature to designate mode shapes $\Psi_n(\mathbf{x})$, instead of $P(\mathbf{x}, \omega_n)$, and/or to report $k_n = \omega_n / c_0$.

If damping is present, then the eigenfrequencies ω_n are complex. The real part of ω_n continues to control the rate of oscillation, but the imaginary part controls the rate of exponential decay as follows:

$$\begin{aligned} p(\mathbf{x}, t) &= \mathrm{Real}\left(\Psi_n(\mathbf{x}) \mathrm{e}^{-\mathrm{i}\omega_n t}\right) \\ &= \mathrm{Real}\left(\Psi_n(\mathbf{x}) \overbrace{\mathrm{e}^{-\mathrm{i}\mathrm{Real}(\omega_n)t}}^{\text{oscillation}} \overbrace{\mathrm{e}^{\mathrm{Imag}(\omega_n)t}}^{\text{exp.decay}} \right). \end{aligned} \tag{3}$$

The second exponential term is non-oscillatory because its exponent is purely real. For this to be a decay, as is physically correct, $\mathrm{Imag}(\omega_n)$ must be negative. It is common to state that modes decay according to $\mathrm{e}^{-\beta_n t}$, where β_n is the decay rate, hence it follows that $\beta_n = -\mathrm{Imag}(\omega_n)$. The units of β_n is Nepers per second; this can be converted to dB per second by multiplication by $20/\ln(10)$. This allows the modal decay rate MT_{60} to be found from β_n, as done by Magalotti and Cardinali [5]. MT_{60} is the time in seconds it takes for the amplitude of a mode to decay by 60dB, hence:

$$\begin{aligned} 60 &= MT_{60,n} \times \beta_n \times \frac{20}{\ln(10)}, \\ MT_{60,n} &= 60 \times \frac{\ln(10)}{20\beta_n} = \frac{3\ln(10)}{\beta_n} \approx \frac{6.908}{\beta_n}. \end{aligned} \tag{4}$$

β_n can be related to Q-factor as follows [9]:

$$Q = \frac{\mathrm{Real}(\omega_n)}{2\beta_n} = -\frac{\mathrm{Real}(\omega_n)}{2\mathrm{Imag}(\omega_n)} \tag{5}$$

The relationships in eq. (4) and (5) between eigenfrequencies and quantities that are critical in the subjective rating of critical listening environments, emphasize the useful role that eigenfrequency analysis can play in their design. They do, however, require the properties of the room boundaries to be known. Note that these relationships have been reported following the $\mathrm{e}^{-\mathrm{i}\omega t}$ time convention in eq. (1). If a $\mathrm{e}^{-\mathrm{i}\omega t}$ convention is followed, then the sign is flipped for all terms involving $\mathrm{Imag}(\omega_n)$.

Eigenfrequency study results can also be used to reconstruct Frequency Response results. The set of eigenmodes $\Psi_n(\mathbf{x})$ form an orthogonal basis with which the spatial distribution of the sound pressure field can be represented. The response $P(\mathbf{x}, \omega)$ produced by a monopole source of frequency ω and volume velocity q m^3/s at position $\mathbf{x}_0$ can be expressed as a sum over modal responses by [10]:

$$P(\mathbf{x}, \omega) = -\mathrm{i}\omega q \rho_0 c_0^2 \sum_{n=0}^{\infty} \frac{\Psi_n(\mathbf{x})\Psi_n(\mathbf{x}_0)}{K_n(\omega_n^2 - \omega^2)}. \tag{6}$$

Here ρ_0 is the density of air and K_n is a normalisation constant that is related to the room volume. $\Psi_n(\mathbf{x}_0)$ is the n^{th} eigenmode evaluated at the source position $\mathbf{x}_0$ and $\Psi_n(\mathbf{x})$ is the same mode shape evaluated at the listener position $\mathbf{x}$. This states the well-known phenomenon that a mode is only excited if the source is on a non-zero part of the mode shape, and only heard if the listener is also on a non-zero part of the mode shape. If either source or receiver is on a spatial null, then the mode will transfer no power between those two locations. The denominator term $\omega_n^2 - \omega^2$ states that modes respond most strongly to excitation close to their natural frequency, so $\omega_n^2 \approx \omega^2$ and $\omega_n^2 - \omega^2 \approx 0$. ω is real, so this occurs most extremely when ω_n has a small imaginary part, following eq. (5).

2.2. Boundary Element Method for the Helmholtz Equation

Room Acoustics problems are *interior problems*, a category for which the acoustic domain Ω is finite and bounded by a closed boundary Γ. $\hat{\mathbf{n}}$ is the boundary surface normal vector, which for an interior problem points out of Ω.

BEM can solve numerically for the pressure field throughout the domain Ω through the meshing of the boundary only. This is performed using a mesh of elements, hence the algorithm's name.

The problem can be represented in the form of a boundary integral equation. Using Green's formula, the sound pressure field $P(\mathbf{x})$ in a room is defined as [6]:

$$P(\mathbf{x}) = \int_{\Gamma} G(\mathbf{x},\mathbf{y}) \frac{\partial P}{\partial n}(\mathbf{y}) d\Gamma_{\mathbf{y}} - \int_{\Gamma} \frac{\partial G}{\partial n}(\mathbf{x},\mathbf{y}) P(\mathbf{y}) d\Gamma_{\mathbf{y}}. \tag{7}$$

Here $G(\mathbf{x},\mathbf{y}) = \mathrm{e}^{\mathrm{i}k|\mathbf{x}-\mathbf{y}|}/4\pi|\mathbf{x}-\mathbf{y}|$ is the free-space acoustic Green's function and $\mathbf{y}$ is a point on the room boundary Γ. $\partial/\partial n$ is shorthand for $\hat{\mathbf{n}} \cdot \nabla$, evaluated at point $\mathbf{y}$. By taking the limit of eq. (7) as $\mathbf{x}$ approaches the boundary, the following relationship is obtained:

$$\frac{1}{2} P(\mathbf{x}) + \mathcal{D}\{P\}(\mathbf{x}) - \mathcal{S}\left\{\frac{\partial P}{\partial n}\right\}(\mathbf{x}) = 0. \tag{8}$$

Here $\mathcal{S}$ and $\mathcal{D}$ are respectively termed the single and double-layer potential operators, which for some argument boundary field $\phi(\mathbf{y})$ are defined:

$$\mathcal{S}\{\phi(\mathbf{y})\}(\mathbf{x}) = \int_{\Gamma} \phi(\mathbf{y}) G(\mathbf{x},\mathbf{y}) d\Gamma_{\mathbf{y}} \tag{9}$$

$$\mathcal{D}\{\phi(\mathbf{y})\}(\mathbf{x}) = \int_{\Gamma} \phi(\mathbf{y}) \frac{\partial G(\mathbf{x},\mathbf{y})}{\partial n} d\Gamma_{\mathbf{y}}. \tag{10}$$

The physical interpretation of the single-layer potential is the pressure at $\mathbf{x}$ caused by particle velocity with a density of $\phi(\mathbf{y})$ emerging through the boundary. Every point on the boundary has a monopole radiation characteristic. The double-layer potential is the pressure field at $\mathbf{x}$ caused by a pressure differential at the boundary with distribution $\phi(\mathbf{y})$. This radiation has a dipole characteristic.

The walls are ascribed an impedance boundary condition with the form:

$$\frac{\partial P}{\partial n} = \mathrm{i}kY_{\mathrm{n}}P. \tag{11}$$

Y_{n} is normalised acoustic admittance, which is found from surface impedance Z_{s} by $Y_{\mathrm{n}} = \rho_0 c_0 / \mathrm{Z_s}$. Substituting eq. (11) into eq. (8), the final boundary integral equation is obtained:

$$\left[\tfrac{1}{2}\mathcal{I} + \mathcal{D} - \mathrm{i}kY_{\mathrm{n}}\mathcal{S}\right]\{P\}(\mathbf{x}) = 0. \tag{12}$$

Usually, one would need to consider source terms in addition to the above, e.g., monopoles within the room or sections of vibrating boundary representing loudspeaker cones. But this is not required for an eigenfrequency solution, which finds mode shapes Ψ_n and frequencies ω_n in the absence of a driving source. These can then be used as a reduced basis with which to compute the frequency response occurring in response to a source, e.g., using eq. (6).

Eq. (12) may be solved in the form of a matrix equation to compute the boundary pressures. Once these are known, eq. (7) can be used to reconstruct the pressure at any point in the domain.

Because the Green's function $G(\mathbf{x},\mathbf{y})$ is at the heart of all the terms in these equations, and because it depends on frequency via k, all the entries in the matrix produced by discretisation of eq. (12) will also depend on ω and k. This drives the need for the eigensolver algorithm that follows.

2.3. Solution of the Eigenproblem using Block SS Method

Eigenfrequency solvers solve internally for wavenumber. They aim to find $k_n = \omega_n/c_0$. But the presence of k in the exponent in the Green's function makes the BEM matrices non-linear in their dependence on k, and therefore on ω too). Modal analysis with BEM, therefore, falls into the category of being a *Non-linear Eigenvalue Problem* (NEP). This takes the general form:

$$\mathbf{A}(k_n)\boldsymbol{\psi}_n = \mathbf{0}. \tag{13}$$

For our problem, $\mathbf{A}$ is the matrix arising from discretisation of eq. (12), k_n is the eigenfrequency as a wavenumber, which we will call the *eigenvalue*, and $\boldsymbol{\psi}_n$ is its corresponding *eigenvector*, which describes the eigenmode $\Psi_n(\mathbf{x})$ via the coefficients of the shape functions in the mesh. Note that no assumption has been made on how $\mathbf{A}$ depends on k. $\mathbf{A}$ is a function of k, but it is not specified how.

To solve the NEP, a contour integral based method, called the block Sakurai-Sugiura (SS) method [11] is used. This converts the NEP into a linear eigenvalue problem smaller in size. This converted problem possesses a set of linear equations that can be solved numerically by standard methods. Together these can form a large system, but they are independent and can be solved in parallel.

The coefficients of this converted problem are computed employing a contour integral in the complex k plane. The integration contour $\mathcal{C}$ must be a positively oriented closed Jordan curve. Here, it is taken to be a circle of radius k_r. This is positioned enclosing the frequency region of interest, centred on a wavenumber k_0. The converted problem is solved for in a translated and scaled complex coordinate $\kappa = (k - k_0)/k_\mathrm{r}$. Eigenvalue / eigenvector pairs $(k_n, \boldsymbol{\psi}_n)$ of the original problem are found from those of the converted problem $(\kappa_n, \mathbf{w}_n)$ by:

$$k_n = k_0 + k_\mathrm{r}\kappa_n, \tag{14}$$

$$\boldsymbol{\psi}_n = \mathbf{S}\mathbf{w}_n. \tag{15}$$

Here $\mathbf{S}$ is the horizontal concatenation of M blocks $\mathbf{S}_m$, that is, $\mathbf{S} = [\mathbf{S}_0, \mathbf{S}_1, \ldots, \mathbf{S}_{M-1}]$, defined as:

$$\mathbf{S}_m = \frac{1}{2\pi\mathrm{i}} \int_{\mathcal{C}} k^m \mathbf{A}(k)^{-1}\mathbf{V}\, dk\,. \tag{16}$$

$\boldsymbol{\psi}_n$ is size $N \times 1$, where N is the number of degrees of freedom in the BEM system. $\mathbf{V}$ is a matrix of size $N \times L$, and can be set arbitrarily so long as its columns are linearly independent. It was set randomly, following [11]. L and M are two integer parameters of the method. Their product, ML, is an upper limit on the number of eigenvalues that will be solved for, and L is the size of each block, which relates to the eigenvalue multiplicity; it should be much smaller than N. $\mathbf{S}$ is therefore size $N \times ML$, and $\mathbf{w}_n$ is size $ML \times 1$.

To find $\mathbf{w}_n$ and κ_n, and the generalised linear eigenvalue problem $\mathbf{G}_{ML}\mathbf{w}_n = \kappa_n \mathbf{H}_{ML}\mathbf{w}_n$ is solved using standard techniques. Here $\mathbf{G}_{ML}$ and $\mathbf{H}_{ML}$ are a pair of Hankel matrices defined as:

$$\mathbf{G}_{ML} = \begin{pmatrix} \mathbf{M}_0 & \cdots & \mathbf{M}_{M-1} \\ \vdots & \ddots & \vdots \\ \mathbf{M}_{M-1} & \cdots & \mathbf{M}_{2M-2} \end{pmatrix} \qquad \mathbf{H}_{ML} = \begin{pmatrix} \mathbf{M}_1 & \cdots & \mathbf{M}_{M} \\ \vdots & \ddots & \vdots \\ \mathbf{M}_{M} & \cdots & \mathbf{M}_{2M-1} \end{pmatrix}. \tag{17}$$

The blocks of these, $\mathbf{M}_m$, are called the moment matrices. They are size $L \times L$ and are defined:

$$\mathbf{M}_m = \frac{1}{2\pi\mathrm{i}} \int_{\mathcal{C}} k^m \mathbf{U}^H \mathbf{A}(k)^{-1}\mathbf{V}\, dk \tag{18}$$

where $\mathbf{U}$ is another matrix satisfying the same criteria as $\mathbf{V}$. They were taken to be equal.

The contour integrals in equations (16) and (18) were calculated using a J-point trapezoidal rule on the circular path $\mathcal{C}$. This amounts to defining abscissa $\kappa_j = \exp(2\pi\mathrm{i}(j + {}^1\!/_2)/J)$. Therefore, $\mathbf{M}_m$ and $\mathbf{S}_m$ are calculated numerically as:

$$\mathbf{M}_m \approx \frac{1}{J}\sum_{j=0}^{J-1} {\kappa_j}^{m+1}\mathbf{U}^H\mathbf{A}(k)^{-1}\mathbf{V}, \tag{19}$$

$$\mathbf{S}_m \approx \frac{1}{J}\sum_{j=0}^{J-1} {\kappa_j}^{m+1}\mathbf{A}(k)^{-1}\mathbf{V}\ . \tag{20}$$

Ref. [11] additionally suggests that a Singular Value Decomposition (SVD) should be performed on $\mathbf{G}_{ML}$ and $\mathbf{H}_{ML}$ before the system is solved, and singular values smaller than a predefined relative threshold δ be excluded. This reduces the number of eigenvalues and eigenmodes that are returned.

3. NUMERICAL EXAMPLES

This section presents two examples applying the block SS method to low frequency acoustic modal analysis of small rooms: a cuboid room and an irregular room, as depicted in Figure 1.

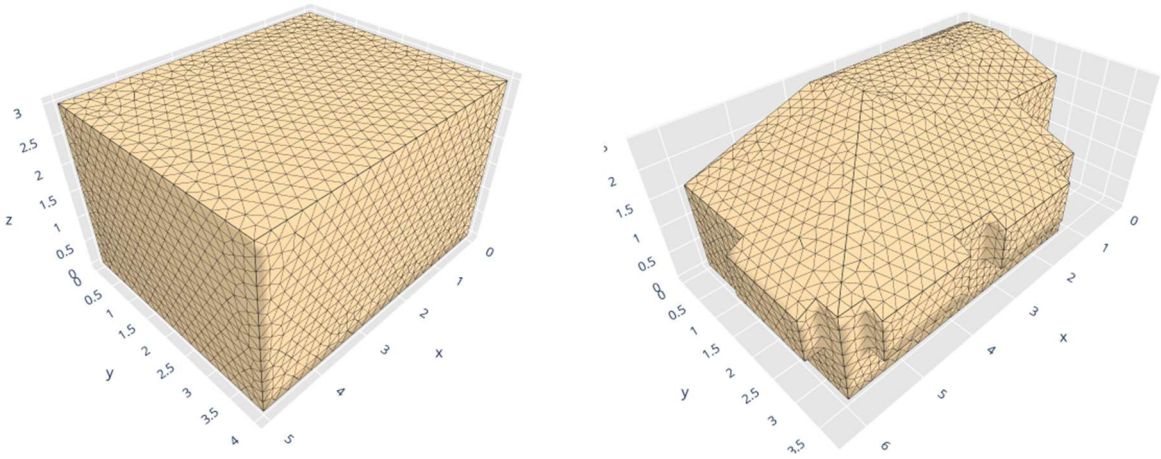

Figure 1: Cuboid room model (left) and irregular room model (right).

The modelling process was as follows:

- The geometries were constructed in STEP [12] format and then imported into GMSH [13] to generate the 3D and 2D meshes for the FEM and BEM models respectively.
- FEM models of each room are computed and used as a reference for the proposed BEM eigensolver. The FEM operators were created using FEniCSx [14] and the FEM eigenproblem was solved using the SLEPc4py Python package. The SLEPc4py solver is set to use the same block SS contour integral based method proposed for BEM [15], but for a *Polynomial Eigenvalue Problem* (PEP), This is done to ensure that the converged eigenvalues are all ones within the integration contour, expediting comparison between BEM and FEM.
- For the BEM models, bempp-cl v0.2.4 is employed [16]. This provides a comprehensive collection of routines for the assembly of boundary integral operators to solve a wide range of problems in several application domains, including Helmholtz problems for scalar acoustics.
- The matrix operators in equation (12) are constructed using bempp-cl, then converted to dense matrices and input into the block SS method algorithm. implemented in SciPy.
- For the cuboid room only, the calculated eigenvalues are compared with the analytical solution provided in equation 4 from Ref. [5].

- Both BEM and FEM used continuous linear piecewise interpolation, for which the number of elements matches the number of the mesh vertices. Notably, the bempp API includes a method *bempp.api.external.fenicsx* that is able to match the approximation space, trace the BEM coefficients to the FEM ones and keep consistency in the post-processing of the results.

The acoustic and meshing parameters for both models were set:

- Air density ρ_0 = 1.21 kg/m^3,
- Speed of sound c_0 = 343 m/s,
- Normalised acoustic admittance Y_n = 0.0125, uniformly distributed on all surfaces,
- Maximum mesh size h = 0.23 m, equivalent to 10 elements per wavelength at 150 Hz.

The block SS method parameters were set:

- Integration path centre k_r = 1.557 + 0i rads/m and radius k_r = 1.374 rads/m,
- Number of contour quadrature points: J = 64,
- Moment size M = 16, estimated as J/4 following [17],
- Block size L = 16,
- Singular value decomposition threshold δ = 10^{-12}.

3.1. Cuboid room

The first numerical example consists of a cuboid room with dimensions 5.0 x 4.0 x 3.0 m (L x W x H), a volume of 60 m^3 and an impedance boundary condition as described above. The boundary mesh includes 4506 elements and 2255 vertices, the latter being the size N of the BEM problem.

The number of converged eigenvalues obtained with the block SS method was 113, but a filter is applied to exclude the fictitious eigenvalues with an imaginary part greater than 0.05 in absolute value. This was deemed to be a realistic upper limit for damping in real rooms [10]. Moreover, the analysis of the results is limited to the first 41 eigenvalues only, for reasons of convenience in the comparison with the results from the FEM model (see section 3.3).

The calculated eigenvalues are listed in Table 1 and shown graphically in Figure 2. Examples of calculated eigenshapes are shown in Figure 3.

Table 1: Calculated eigenvalues for the cuboid room BEM model.

n	k_n	n	k_n	n	k_n	n	k_n
1	0.6283 - 0.0123i	12	1.6918 - 0.0154i	23	2.2679 - 0.0194i	34	2.6333 - 0.0153i
2	0.7854 - 0.0129i	13	1.8146 - 0.0195i	24	2.2950 - 0.0195i	35	2.6540 - 0.0195i
3	1.0058 - 0.0154i	14	1.8850 - 0.0122i	25	2.3234 - 0.0194i	36	2.6678 - 0.0195i
4	1.0472 - 0.0139i	15	1.8879 - 0.0170i	26	2.3562 - 0.0128i	37	2.6704 - 0.0153i
5	1.2212 - 0.0164i	16	1.9897 - 0.0195i	27	2.4386 - 0.0152i	38	2.6924 - 0.0195i
6	1.2567 - 0.0123i	17	2.0117 - 0.0154i	28	2.4425 - 0.0164i	39	2.7228 - 0.0163i
7	1.3090 - 0.0171i	18	2.0421 - 0.0154i	29	2.4535 - 0.0157i	40	2.8177 - 0.0164i
8	1.4520 - 0.0196i	19	2.0945 - 0.0139i	30	2.5134 - 0.0122i	41	2.8339 - 0.0195i
9	1.4819 - 0.0154i	20	2.1561 - 0.0164i	31	2.5657 - 0.0195i		
10	1.5708 - 0.0129i	21	2.1866 - 0.0165i	32	2.5785 - 0.0170i		
11	1.6358 - 0.0164i	22	2.2370 - 0.0170i	33	2.6180 - 0.0170i		

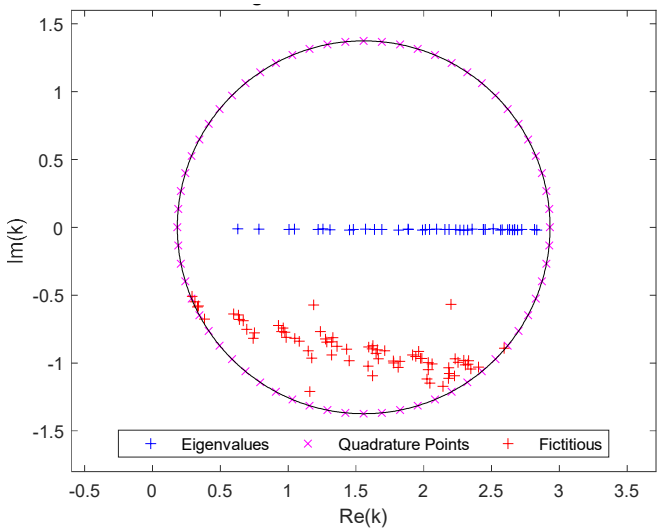

Figure 2: Eigenvalues in the complex wavenumber plane for the cuboid room BEM model.

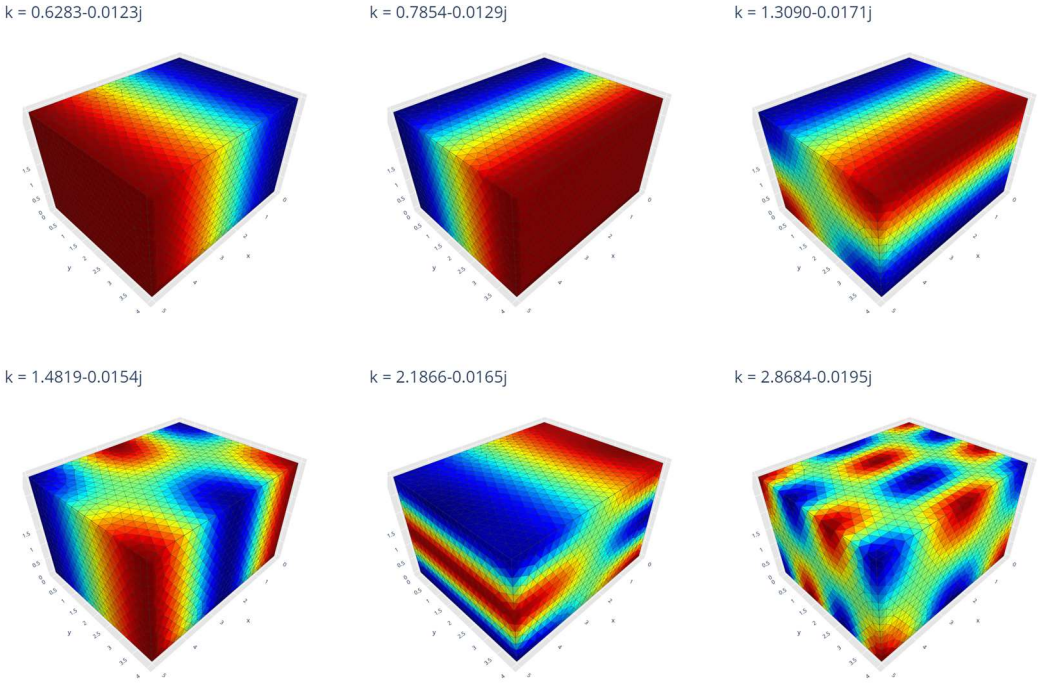

Figure 3: Examples of calculated eigenshapes for the cuboid room model (red = positive pressure, blue = negative pressure, green = zero pressure).

3.2. Irregular room

The second numerical example consists of a non-regularly shaped room, characterised by an L-shaped floor plan and a pitched roof with perpendicular folds and a flat portion. The dimensions of the maximum external dimensions are 6.2 x 3.8 x 2.4 m (L x W x H), room volume of 39 m^3 and impedance boundary conditions as described above. The boundary mesh features 4596 elements and 2298 vertices, the latter being the number of degrees of freedom N in the BEM problem. In the same fashion as the previous example, the number of converged eigenvalues is 90, however, 33 have been filtered based on the imaginary part and 31 only have been considered for the result analysis. The eigenvalues are listed in Table 2 and shown graphically in Figure 4. Examples of the calculated eigenshapes are shown in Figure 5.

Table 2: Calculated eigenvalues for the irregular room BEM model.

n	k_n	n	k_n	n	k_n	n	k_n
1	0.5534 - 0.0158i	9	1.7191 - 0.0177i	17	2.1902 - 0.0257i	25	2.6267 - 0.0166i
2	0.8949 - 0.0166i	10	1.7714 - 0.0182i	18	2.2667 - 0.0205i	26	2.6632 - 0.0212i
3	0.9735 - 0.0167i	11	1.8857 - 0.0190i	19	2.2974 - 0.0203i	27	2.7039 - 0.0210i
4	1.1946 - 0.0171i	12	1.9366 - 0.0201i	20	2.3946 - 0.0218i	28	2.7162 - 0.0194i
5	1.4121 - 0.0203i	13	1.9776 - 0.0198i	21	2.4636 - 0.0229i	29	2.8078 - 0.0191i
6	1.4774 - 0.0160i	14	2.0225 - 0.0163i	22	2.5463 - 0.0187i	30	2.8275 - 0.0226i
7	1.5646 - 0.0203i	15	2.0716 - 0.0229i	23	2.5586 - 0.0211i	31	2.8404 - 0.0233i
8	1.6444 - 0.0203i	16	2.1532 - 0.0199i	24	2.5828 - 0.0207i		

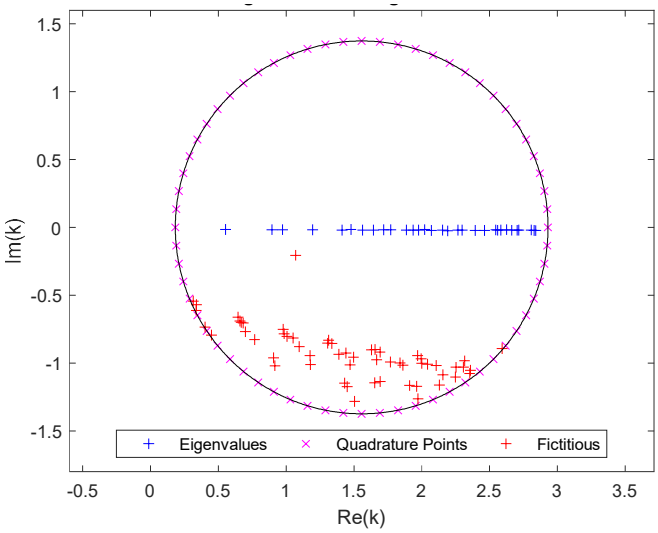

Figure 4: Eigenvalues in the complex wavenumber plane for the irregular room BEM model.

3.3. Comparison with FEM

To compare the eigenmodes and eigenfrequencies between BEM and FEM, the Modal Assurance Criterion (MAC) [18] was used to ensure correct matches. This provides a measure of assurance that describes the spatial correlation between pairs of eigenmode shapes in energetic terms. For the specific case, the MAC has been formulated in a quasi-continuous spatial sense as:

$$\mathbf{MAC}(i,j) = \frac{\left|\boldsymbol{\Psi}_{FEM,i}^{\mathrm{H}}\mathbf{I}_{BEM2FEM}\boldsymbol{\Psi}_{BEM,j}\right|^2}{\left(\boldsymbol{\Psi}_{FEM,i}^{\mathrm{H}}\mathbf{I}_{FEM2FEM}\boldsymbol{\Psi}_{FEM,i}\right)\left(\boldsymbol{\Psi}_{BEM,j}^{\mathrm{H}}\mathbf{I}_{BEM2BEM}\boldsymbol{\Psi}_{BEM,j}\right)}. \tag{21}$$

Here $\boldsymbol{\Psi}_{FEM,i}$ is the i$^{\text{th}}$ FEM eigenshape (at the room boundary only), $\boldsymbol{\Psi}_{BEM,j}$ is the j$^{\text{th}}$ BEM eigenshape, $\mathbf{I}_{BEM2FEM}$ is the trace mass matrix to map BEM coefficients to FEM ones, $\mathbf{I}_{FEM2FEM}$ is the FEM mass matrix and $\mathbf{I}_{BEM2BEM}$ is the BEM mass matrix.

The **MAC** values are constrained between 0 and 1, with 1 representing perfect correlation. Ones on the diagonal of the matrix indicates matching mode ordering too. The **MAC** plots for the evaluated models are shown in Figure 6, showing good agreement between BEM and FEM simulations.

The average residuals on the **MAC** matrices diagonal are 6.5×10^{-4} and 6.7×10^{-2} for the cuboid and irregular rooms respectively.

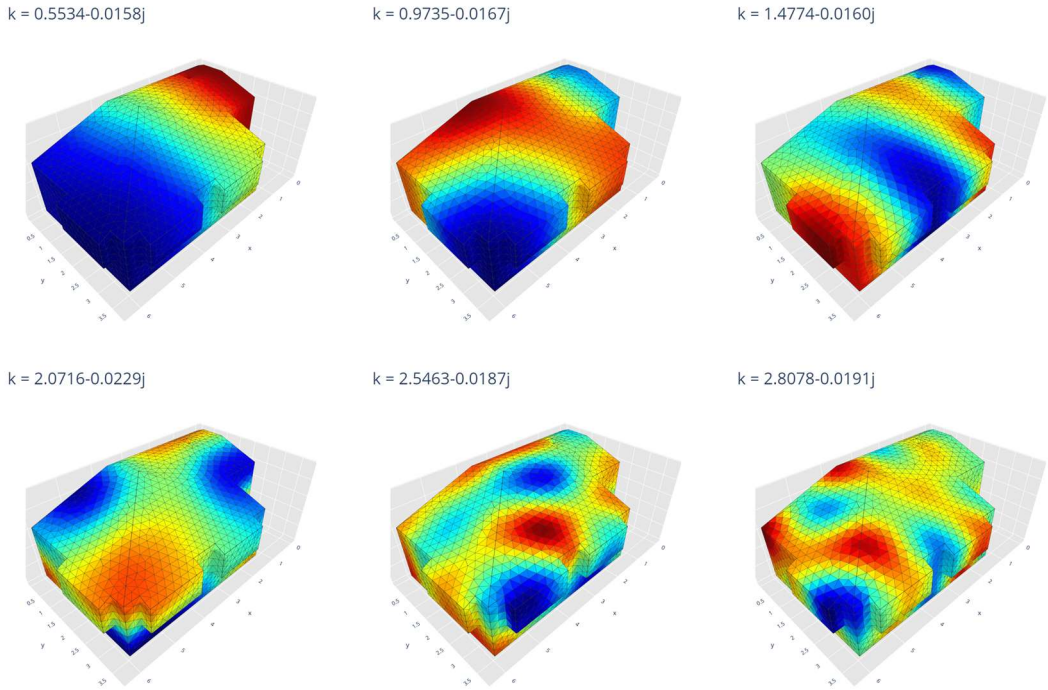

Figure 5: Examples of calculated eigenshapes for the irregular room model (red = positive pressure, blue = negative pressure, green = zero pressure).

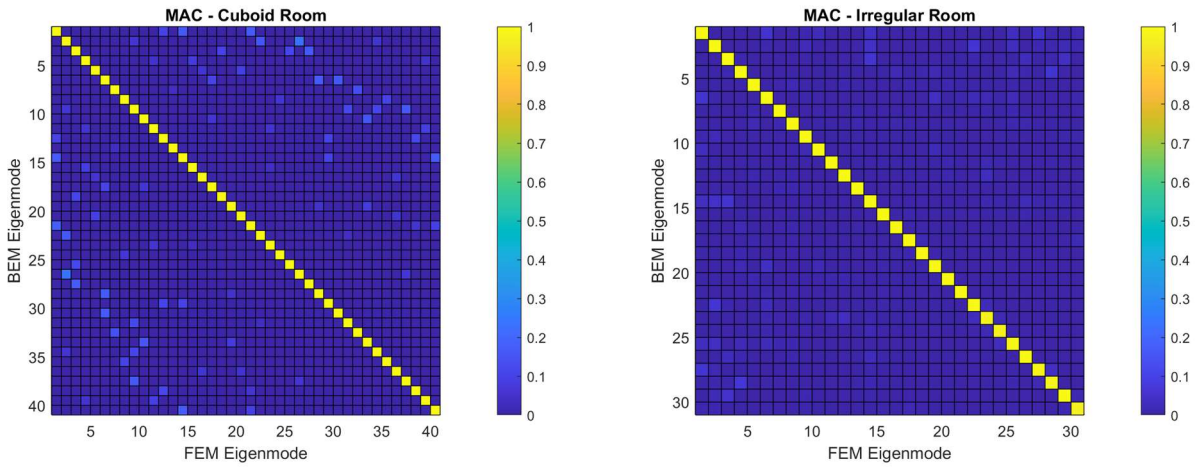

Figure 6: **MAC** plots for the evaluated models.

Figure 7 compares the eigenvalues computed by BEM and FEM. For the cuboid room, a set calculated using an analytical model (eq. 4 in [5]) is also shown for validation purposes.

It is seen that the eigenvalues computed with BEM match the analytical model well throughout for the cuboid room, but that the ones from FEM drift upward in frequency ($\equiv \mathrm{Real}(k)$) and toward higher damping ($\equiv \mathrm{Imag}(k)$), and that this effect increases with frequency.

This trend arises from a common phenomenon in FEM called *pollution error*. As discussed in section 1, this increases the effective numerical wave speed and thus, in eigenfrequency problems, over-predicts the eigenfrequency. These results show that it also compromises the imaginary part of eigenfrequency for FEM, which controls both the decay rate of modes and the Q-factor. This issue can also affect the eigenvalue search when using a contour integral based method with FEM, as the shift of the real part causes some of the solutions to fall outside the integration path.

BEM, in contrast, is built upon a fundamental solution of the Helmholtz equation – the free-space Green's function – that has propagation speed embedded in its definition. This allows it to avoid pollution error, so it can provide accurate eigenfrequency results over a wider bandwidth.

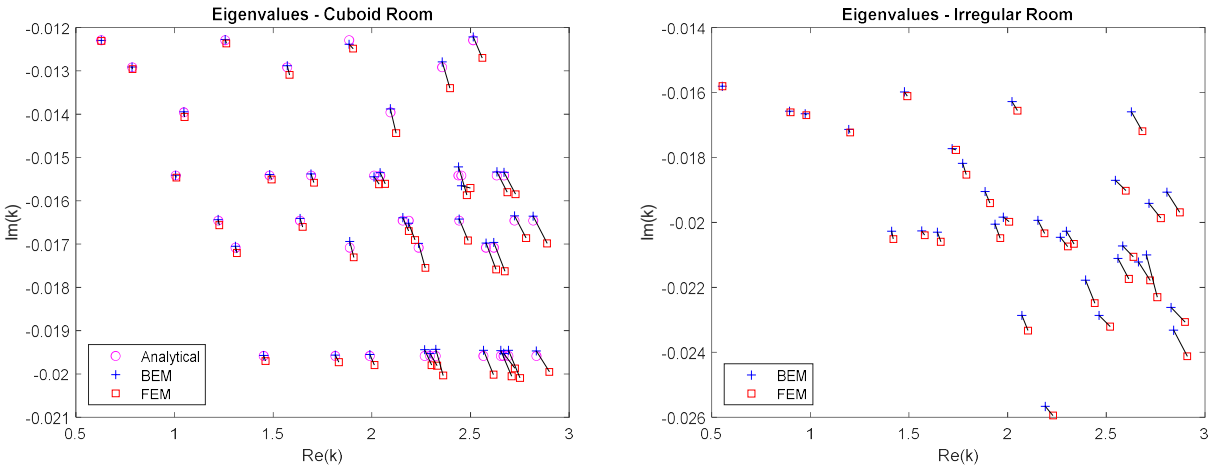

Figure 7: Eigenvalue comparison between BEM and FEM for the evaluated models, and an analytical model for the cuboid room. The black lines connect eigenvalues with the same index.

Figure 8 shows the trend more clearly by plotting the relative error of the eigenvalues computed using FEM and BEM for the cuboid room, compared to the analytical model. The improved performance of BEM relative to FEM is particularly obvious in the real part of high index eigenvalues (left plot), as the relative error for FEM presents a polynomial upward trend as frequency increases, whereas the error for BEM reduces with frequency. For the imaginary part, the error for FEM follows the same trend, albeit less smoothly. The BEM error follows this upward trend too, but an order of magnitude lower.

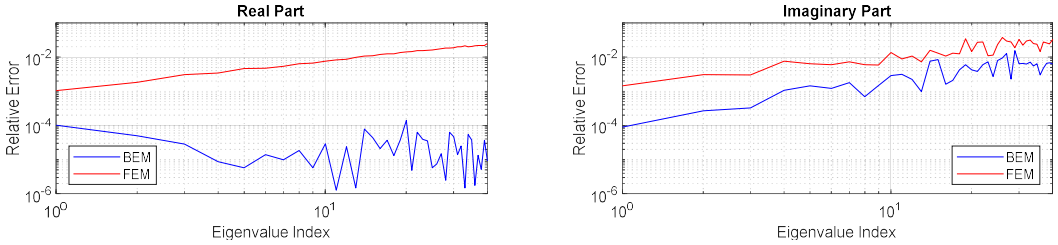

Figure 8: Relative error on the real (left) and imaginary (right) parts of the BEM and FEM eigenvalues to the analytical solution.

4. CONCLUSION

This paper reports a novel approach to performing modal analysis for room acoustics applications, using BEM and a contour integral based algorithm for the solution of the non-linear eigenproblem.

The proposed method is validated against the results obtained from a reference analytical model and models constructed in FEM. FEM generally lends itself better to eigenfrequency study because the matrix coefficients are independent of frequency. But the results presented here indicate that the BEM eigenfrequency algorithm has the potential to be more accurate at high frequencies than its accepted FEM counterpart, due to the absence of pollution error. Moreover, since it makes no assumptions about the dependence of the model on frequency, it can also include arbitrary frequency-dependent boundary conditions, such as boundary admittance, which the standard solvers used for FEM cannot.

Results are obtained for two rooms with different shapes – cuboid and irregular – and good agreement is found with FEM results for both the eigenvalues and eigenshapes.

The proposed method has the drawback of fictitious eigenvalues being computed, although these are easily recognizable by the imaginary part being significantly higher in absolute value and hence can be readily filtered out.

Further work includes exploration of different integration paths and the optimisation of the block SS parameters to make the new method more effective, and more computationally efficient, for the room acoustics application proposed.

5. REFERENCES

[1] S.E. Olive, P.L. Schuck, J.G. Ryan, S.L. Sally, M.E. Bonneville, The detection thresholds of resonances at low frequencies, Journal of the Audio Engineering Society. 45 (1997) 116–128.

[2] M.R. Avis, B.M. Fazenda, W.J. Davies, Thresholds of detection for changes to the Q factor of low-frequency modes in listening environments, AES: Journal of the Audio Engineering Society. 55 (2007) 611–622.

[3] B.M. Fazenda, L.A. Elmer, M. Wankling, J.A. Hargreaves, J.M. Hirst, Subjective preference of modal control in listening rooms, 129th Audio Engineering Society Convention 2010. 1 (2010) 496–507.

[4] B.M. Fazenda, M. Stephenson, A. Goldberg, Perceptual thresholds for the effects of room modes as a function of modal decay, J Acoust Soc Am. 137 (2015) 1088–1098. https://doi.org/10.1121/1.4908217.

[5] R. Magalotti, V. Cardinali, Building FEM low frequency room models through modal decay time measurements, Proceedings of the International Congress on Acoustics. 2019-Septe (2019) 4081–4087.

[6] P. D'Antonio, R. Petrolli, J. Storyk, J.A. Hargreaves, T. Betcke, Non-cuboid iterative room optimizer, in: J Acoust Soc Am, Lyon, 2020: pp. 2798–2798. https://doi.org/10.1121/1.5147791.

[7] S. Marburg, A pollution effect in the boundary element method for acoustic problems, Journal of Theoretical and Computational Acoustics. 26 (2018) 1–18.

[8] S.N. Chandler-Wilde, E.A. Spence, A. Gibbs, V.P. Smyshlyaev, High-frequency Bounds for the Helmholtz Equation Under Parabolic Trapping and Applications in Numerical Analysis, SIAM Journal on Mathematical Analysis. 52 (2020) 845–893. https://doi.org/10.1137/18M1234916.

[9] L. Kinsler, A. Frey, A. Coppens, J. Sanders, Fundamentals of acoustics, 4th ed., Wiley, New York, 2000.

[10] H. Kuttruff, Room Acoustics, 5th ed., London, 2002. https://doi.org/10.1201/9781482286632.

[11] J. Asakura, T. Sakurai, H. Tadano, T. Ikegami, K. Kimura, A numerical method for nonlinear eigenvalue problems using contour integral, Japan Journal of Industrial and Applied Mathematics. 27 (2010) 73–90. https://doi.org/10.1007/s13160-010-0005-x.

[12] ISO, Industrial automation systems and integration — Product data representation and exchange — Part 242: Application protocol: Managed model-based 3D engineering, Iso 10303-242. (2020). https://www.iso.org/standard/66654.html.

[13] C. Geuzaine, J.-F. Remacle, Gmsh: A 3-D finite element mesh generator with built-in pre- and post-processing facilities, International Journal for Numerical Methods in Engineering. 79 (2009) 1309–1331. https://doi.org/10.1002/nme.2579.

[14] C.N.R. M. W. Scroggs J. S. Dokken, G.N. Wells, Construction of arbitrary order finite element degree-of-freedom maps on polygonal and polyhedral cell meshes, 2022.

[15] Y. Maeda, T. Sakurai, J.E. Roman, Contour Integral Spectrum Slicing Method in SLEPc, 2016. https://slepc.upv.es/documentation/reports/str11.pdf.

[16] T. Betcke, M.W. Scroggs, Bempp-cl: A fast Python based just-in-time compiling boundary element library, Journal of Open Source Software. 6 (2021) 2879. https://doi.org/10.21105/joss.02879.

[17] T. Sakurai, Y. Futamura, H. Tadano, Efficient parameter estimation and implementation of a contour integral-based eigensolver, Journal of Algorithms and Computational Technology. 7 (2013) 249–270. https://doi.org/10.1260/1748-3018.7.3.249.

[18] M. Pastor, M. Binda, T. Harčarik, Modal Assurance Criterion, Procedia Engineering. 48 (2012) 543–548. https://doi.org/10.1016/j.proeng.2012.09.551.